

6p valence relativistic effects in 5d photoemission spectrum of Pb atom and bonding properties of Pb-dimer using Dirac-Hartree-Fock formalism including many-body effects

Cite as: J. Vac. Sci. Technol. A 40, 043205 (2022); <https://doi.org/10.1116/6.0001888>

Submitted: 26 March 2022 • Accepted: 13 May 2022 • Published Online: 07 June 2022

 Paul S. Bagus and  Sefik Suzer

COLLECTIONS

Paper published as part of the special topic on [Commemorating the Career of David Arthur Shirley](#)



View Online



Export Citation



CrossMark

ARTICLES YOU MAY BE INTERESTED IN

[Perspectives on UV and x-ray photoelectron spectroscopy](#)


Journal of Vacuum Science & Technology A 40, 043002 (2022); <https://doi.org/10.1116/6.0001856>

[Uppsala and Berkeley: Two essential laboratories in the development of modern photoelectron spectroscopy](#)


Journal of Vacuum Science & Technology A 40, 043207 (2022); <https://doi.org/10.1116/6.0001879>

[Half-century old Berkeley idea now finding missing links of nuclear quadrupole moments](#)

Journal of Vacuum Science & Technology A 40, 042802 (2022); <https://doi.org/10.1116/6.0001877>



HIDEN
ANALYTICAL




Instruments for Advanced Science

- Knowledge,
- Experience,
- Expertise

Click to view our product catalogue


Contact Hiden Analytical for further details:
www.HidenAnalytical.com
info@hideninc.com

Gas Analysis




- dynamic measurement of reaction gas streams
- catalysis and thermal analysis
- molecular beam studies
- dissolved species probes
- fermentation, environmental and ecological studies

Surface Science




- UHVTPD
- SIMS
- end point detection in ion beam etch
- elemental imaging - surface mapping

Plasma Diagnostics



- plasma source characterization
- etch and deposition process reaction kinetic studies
- analysis of neutral and radical species

Vacuum Analysis



- partial pressure measurement and control of process gases
- reactive sputter process control
- vacuum diagnostics
- vacuum coating process monitoring

6p valence relativistic effects in 5d photoemission spectrum of Pb atom and bonding properties of Pb-dimer using Dirac–Hartree–Fock formalism including many-body effects

Cite as: J. Vac. Sci. Technol. A 40, 043205 (2022); doi: 10.1116/6.0001888

Submitted: 26 March 2022 · Accepted: 13 May 2022 ·

Published Online: 7 June 2022



View Online



Export Citation



CrossMark

Paul S. Bagus^{1,a)}  and Sefik Suzer^{2,a)} 

AFFILIATIONS

¹Center for Advanced Scientific Computing and Modeling (CASCaM), Department of Chemistry, University of North Texas, 1155 Union Circle #305070, Denton, Texas 76203-5017

²Chemistry Department, Bilkent University, 06800 Ankara, Turkey

Note: This manuscript is a part of the Special Topic Collection Commemorating the Career of David Arthur Shirley.

a) Authors to whom correspondence should be addressed: paul.bagus@unt.edu and suzer@fen.bilkent.edu.tr

ABSTRACT

There has been strong recent interest related to the large spin–orbit coupling in Pb monolayers on various properties of graphene and other 2D-materials. The underlying physical/chemical origin of the spin–orbit splitting has been discussed in terms of the valence 6p atomic level of the lead atom. Indeed, the photoelectron spectra of the Pb atom were the subject of investigations about 50 years ago in Dave Shirley’s laboratory at UC Berkeley. In a paper published in 1975, using He-I UV photoelectron spectroscopy, we reported an unexpected relative intensity ratio for the observed atomic Pb peaks ($^2P_{1/2}$ and $^2P_{3/2}$) after removal of a 6p valence electron and attributed it to the large spin–orbit interaction in that level. In this contribution, we use the Dirac–Hartree–Fock formalism to reanalyze the complex spectral features reported five years later, for the 5d He-II UV photoelectron spectrum of atomic lead, to extract the 6p valence contribution, which turns out to be significant. Furthermore, we calculate the energy levels of the Pb-dimer at the experimental equilibrium geometry of the molecule to also find the significant contribution of the spin–orbit splitting of the atomic 6p levels in the composition of the valence molecular orbitals of the dimer. Such an approach can be extended to larger systems like monolayers containing lead or other heavy atoms, thus helping in designing 2D-materials with controlled and better targeted properties.

Published under an exclusive license by the AVS. <https://doi.org/10.1116/6.0001888>

I. INTRODUCTION

Spin–orbit coupling (SOC) is a relativistic effect that has a very dominant atomic nature but also leads to significant chemical and physical changes on numerous properties of atoms, molecules, solids, and materials.^{1–4} In the first half of the 1970s, research efforts in the late David Shirley’s group involved the use of electron spectroscopic techniques to investigate the electronic properties of various gases, molecules, and solids. These efforts were orchestrated by Shirley himself. One of the authors (S.S.), being a Ph.D. student then, had carried out measurements on vapors generated through a home-built high-temperature oven by recording the photoemitted electrons using an He-I (21.2 eV) light source.⁵ Lead (Pb) was one

of the investigated atoms, which has relatively large vapor pressure at reasonable temperatures (~ 700 °C), and yielded a very interesting valence shell spectrum after the removal of a 6p electron, where the intensity of the remaining $^2P_{1/2}$ ($6p_{1/2}$)¹ component was more than 1 order of magnitude larger than that of the $^2P_{3/2}$ ($6p_{3/2}$)¹ one.⁶

The accepted configuration of the electronic ground state of the Pb atom ($Z=82$) is $6s^26p^2$, which is an open shell electronic system with a very large spin–orbit coupling in the 6p level. The spectroscopic consequences of a large SOC for the general p^2 configuration systems can be understood within a framework where the coupling of the open shell electrons is considered in terms of LS , $j-j$, and intermediate coupling.^{7,8} These different

couplings have been treated within a perturbation theory approach, which has been used to successfully assign the resulting atomic energy levels.⁹ The *LS* coupling scheme dictates that the ground state of Pb with two open shell electrons should be the Russell–Saunders multiplet 3P , and from Hund’s third rule, the lowest energy level will be 3P_0 .⁷ On the other hand, *j-j* coupling would lead to a closed shell $J = 0$ configuration, $(6p_{1/2})^2$. One way of introducing intermediate coupling is to treat spin–orbit interaction as a perturbation and, hence, allow mixing of Russell–Saunders multiplets for levels with the same J value. For an $(np)^2$ configuration, the ground state level becomes a mixture of (3P_0) and (1S_0) with an increasing contribution from the latter as the spin–orbit splitting is increased. It is also possible to start from the *j-j* coupling limit and express the ground state level as a linear combination [$c_1 (6p_{1/2})^2 + c_2 (6p_{3/2})^2$], with increasing c_1 contribution upon increasing SOC constant. In the limit of very large SOC constant, $c_1 = 1$ and $c_2 = 0$. Using the experimental intensities, it was determined that the ground state of Pb is much closer to the *j-j* limit with $(c_2/c_1)^2 = 0.07$, i.e., with 93% $(6p_{1/2})^2$ configuration.⁶ The composition of the ground Pb level is displayed in Fig. 1 where our early results are compared to our present relativistic calculations, discussed further below, on the Pb atom. The early results were obtained from our interpretation of the Pb He-I ultraviolet photoemission data. The new calculations are fully consistent with our earlier conclusion about the composition of the Pb ground level. Our finding for the composition of the Pb level is also in very good agreement

with the relativistic Dirac–Hartree–Fock (DHF) calculations, published three years before our early paper.¹⁰

Similar intensity reversal due to the spin–orbit coupling was also used to reinterpret the already published valence UV photoelectron spectra of the group VI diatomic molecules, having a formal ground electronic state of $(\pi)^2$ configuration.¹¹

Almost in the same era, the late Professor Kenneth Pitzer, another eminent faculty member of the UC Berkeley–Chemistry, published a paper on the bonding trends of the Group IV elements (C, Si, Ge, Sn, and Pb) and boldly claimed that the next group member, a super heavy atom with atomic number 114 (Flerovium), which was hitherto unknown, should be relatively inert and display noble gas properties, since its ground state $(7p)^2$ is expected to be almost pure $(7p_{1/2})^2$, hence, a closed shell system.¹² His hypothesis was later proven to be correct, upon nuclear syntheses of the super heavy elements up to $Z = 118$.^{13–16}

Other papers from Pitzer and his co-workers had reported on the extensive role of the different relativistic effects, rather than just a simple spin–orbit perturbation approach, and pointed out the widely different bonding characteristics of the $6p_{1/2}$ spinors compared to those of the $6p_{3/2}$ ones.^{17–19} Furthermore, relativistic radial contraction and its consequences on bonding properties were determined by carrying out detailed calculations and analysis of several simple molecules having Au through Bi atoms in their structure. The implications of the orbital contraction were also attributed to the different spin–orbit components to have different radial distributions. In fact, one of the authors of the present paper (P.B.S.) was also involved on elucidating effects of the relativity and of the lanthanide contraction on the very same atoms from Hf to Bi, together with Pitzer.²⁰ Bagus also has important collaborations with Shirley’s group on spectroscopic manifestations of the breakdown of the single configuration description, accounting for the observed fine electronic structure in the photoemission spectra of various molecules and solids.^{21,22}

Meanwhile, Pyykko and others have extended this line of research and established a myriad of chemical/physical properties of materials, stemming from relativistic effects.^{3,4,23,24} One very striking example is the paper by Ahuja and co-workers, where they had claimed that the relativistic effects account for the 1.7–1.8 V of the working electrochemical voltage (2.1 V) of the Pb-acid batteries.²⁵ Other observations included higher stability of the lower oxidation (+2) state of Pb, existence of Hg in the liquid form, and yellow color of the metallic Au, together with the unique and interesting chemistry of Au (aurophilicity).^{26,27}

A recent surge of assignments for Pb relativistic effects, naïvely called spin–orbital properties of the Pb atom, has found a new niche within the colossal research activities on graphene and 2D-materials and their applications, since it has been claimed that the large SOC of Pb imparts very favorable effects on these materials, such as inducing (i) electron confinement, (ii) bandgap insertion, (iii) photoinduced charge transfer, etc.^{28–30} However, in most of these papers, assessment of the effect of the atomic SOC of Pb has not been explicitly indicated, except for the work of Ma and Yang, published in 2011.³¹ Those authors had carried out first-principles calculations of Pb doping into defective graphene by adsorbing monomeric and dimeric lead, and extracting the charge transferred to the carbon network. Spin–orbit coupling was

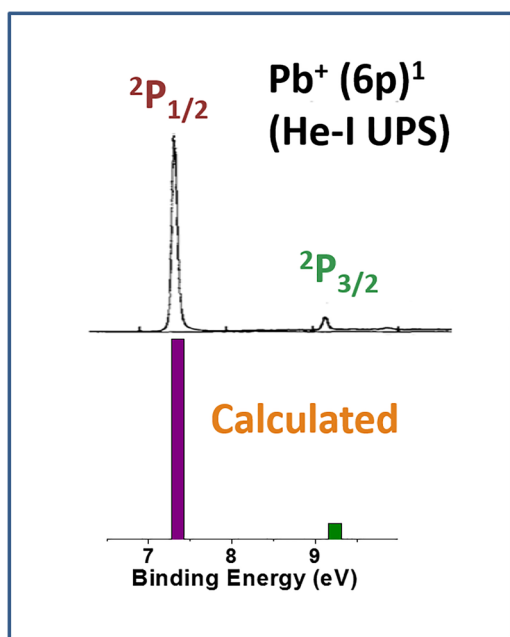


FIG. 1. Assignment of the composition of the ground $J = 0$ atomic Pb level obtained from the He-I UP spectrum of the Pb atom (Refs. 5 and 6), and with our present calculation of the Pb WF. Adopted with permission from Suzer *et al.*, J. Chem. Phys. 63, 3473 (1975). Copyright 1975, AIP Publishing LLC.

introduced using a relativistic density-functional theory calculation, which was found to cause a fivefold increase of the Bychkov–Rashba parameter (α_R)³² for Pb atom, compared to the Sn atom, which is in the same group but one row above Pb in the periodic table.

Since a combination of electrostatic, magnetic, and van der Waals forces are amalgamated when molecules and/or solids are formed, we now ask the question: “*What relativistic effects exactly have been preserved and to what extent, in going from the isolated gas phase Pb atoms to molecules and/or solids containing them?*” For example, in addition to different coupling schemes of the spin and orbital angular momenta, changes in the geometrical environment of the atom within the molecular system introduce strong perturbations, which can be addressed within the ligand-field-theory, including the many-body effects.³³

After his Berkeley years, Suzer had continued working with electron spectroscopy using slightly higher photon energy of 40.8 eV (He-II) to extend the investigation to inner valence levels. In one of his papers, spectra of Hg, Tl, and Pb atoms after photoionization of the closed 5d shell were shown to reveal a complex multiplet structure only for the Pb atom.³⁴ In that work, no clear explanation was provided as to the nature of this complex structure, besides a simple assignment of the peaks using the tables of the atomic energy levels.⁹ In line with the question raised above (i.e., *what properties are preserved?*), we now ask two new questions: (i) “*What is the origin of the satellites which must arise because the 6p shell is open? Are they from 5d_{5/2} or 5d_{3/2} or both?*” and (ii) “*Does the occupation of the 6p change greatly from being dominantly (6p_{1/2})²?*” However, due to the large relativistic effects of both the 6s and 6p orbitals, and in terms of orbital contraction and/or the spin–orbit interaction, we thought that it is worth to explore and test this hypothesis.

Therefore, we reexamine this spectrum with the help of relativistic calculations and trace the contribution(s) of the ground state electronic configuration due to the strong relativistic effects (i.e., mainly 6p_{1/2} nature) in the (5d)^{−1} spectroscopic manifold.

Second, we carry out similar relativistic calculations on both Pb atom and Pb₂-dimer, again to trace the same relativistic effects in the orbital makeup of the molecule with the hope of finding trends that could be extended to complex surface structures like a graphene layer on metal substrates containing a Pb-monolayer in between.

II. EXPERIMENTAL DETAILS

21.1 eV He-I UV photoelectron spectrum of the valence levels (6s and 6p) of lead was recorded in Dave Shirley’s lab in Berkeley using a Perkin-Elmer PS-18 spectrometer modified with a home-built Knudsen evaporation oven for temperatures up to 1000 °C. For Pb, temperatures around 700 °C was used, and the energy calibration was done by introducing Ar and Xe gas with the sample in a separate run. Details of the experimental setup and data gathering can be found in Refs. 5 and 6. 40.8 eV He-II UV PE spectrum was recorded later in Freiburg University, Germany, using a spherical sector electron spectrometer and a high-temperature oven, equipped with a commercial discharge lamp optimized for the He-II radiation (Jobin Yvon Co., France). Details of the experimental setup and data gathering can be found in Ref. 34.

III. COMPUTATIONAL DETAILS

The theoretical results for the properties of the Pb atom and the Pb₂-dimer are based on fully relativistic wave-functions (WFs), for these systems. The DHF orbitals and the total many-electron WFs were determined with the Dirac–Coulomb Hamiltonian,³⁵ where scalar and spin–orbit relativistic effects were taken into account. The four component orbitals were determined for the average of configurations for the open shell systems,^{35,36} and the total many-electron WFs were computed with a complete open shell configuration interaction (COSCI) formalism. In the COSCI formalism, the open shell electrons are distributed in all possible ways over the set of orbitals that can be formed from the closed shell electrons; this set of orbitals is described as the active orbital space for the configuration interaction. For the atom, the six 6p spin–orbitals are in the active space, while for the dimer, 12 spin–orbitals are in the active space.

In nonrelativistic notation, these are the bonding σ_g and π_u and the antibonding σ_u and π_g orbitals. The COSCI WFs have the exact symmetry properties for these open shell systems.³⁶ For the atoms, J is a good quantum number, and for the dimer, Ω is a good quantum number; for the molecular symmetries, see, for example, Herzberg.³⁷ Once spin–orbit splitting is taken into account, L and S for Pb atoms, or Λ and S for diatomic Pb₂, are no longer good quantum numbers. As long as the spin–orbit coupling is small, L and S are good approximations but, as we will show below, for systems with heavy atoms they are not good approximations. Large core, 60 electron effective core potentials (ECPs) are used to describe the Pb atom and only the 5s, 5p, 5d, 6s, and 6p electrons are treated explicitly. Large basis sets are used to represent the orbitals. All integrals are computed exactly except for the class of integrals connecting the small component basis functions with other small component functions that are approximated.³⁵ The orbitals and WFs are calculated with the DIRAC program system,³⁸ and the basis sets and ECP parameters are taken from Refs. 39 and 40.

The relative XPS intensities are obtained with the sudden approximation (SA);^{41,42} for details of the application of the SA to XPS spectra, see Refs. 22, 43 and 44. This approximation is valid for the intensities due to ionization with photons with energies greater than ~200 eV above threshold.⁴⁵ For the UV photon energies used for the work described in the present paper, the SA intensities are only a rough guide since they neglect the photon energy dependence of the photoionization.

TABLE I. Tabulated atomic energy levels (in eV) of Si, Sn, and Pb, and calculated ones for only Pb.

Term	J	Si-3p ² ΔE^a	Sn-5p ² ΔE^a	Pb-6p ² ΔE^a	Pb-6p ² ΔE -theory
3P	0	0.00	0.00	0.00	0.00
	1	0.010	0.21	0.97	0.83
	2	0.028	0.43	1.32	1.30
1D	2	0.78	1.07	2.66	2.70
1S	0	1.91	2.13	3.65	4.05

^aSee Ref. 9.

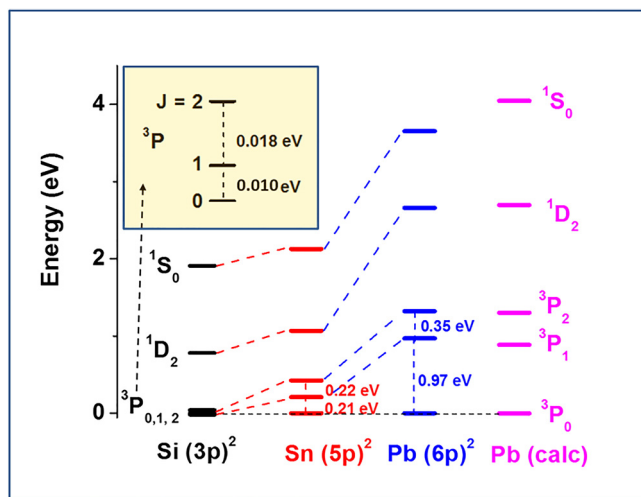


FIG. 2. Experimentally determined energy levels of Si, Sn, and Pb atoms together with the calculated ones for the Pb atom. The inset displays the corresponding energy levels of the Si atom enlarged by a factor of 10 for a better comparison. All data are taken from Ref. 9.

IV. RESULTS AND DISCUSSION

A. Relativistic effects in the valence levels of Si, Sn, and Pb atoms

Si ($3p^2$, $Z=12$), Sn ($5p^2$, $Z=50$), and Pb ($6p^2$, $Z=82$) are members of the group IV elements with widely different spin-orbit coupling constants (ξ) in the valence np levels. The magnitude of the SOC constants extracted from their tabulated energy levels [$\xi = \Delta E(^3P_2 - ^3P_0)$] are 0.028, 0.43, and 1.32 eV for the Si, Sn, and Pb atoms, respectively.⁹ As a result, while a silicon atom can be considered to be almost purely LS coupled, and tin is intermediate, lead must be approaching the $j-j$ limit. The corresponding experimentally determined energies of the resulting multiplets are given in Table I and are also reproduced in Fig. 2. In the same figure, we also include our calculated values for the energies of the dominant composition of the Pb atom. It is seen that the calculated relative energies are in reasonably good agreement with the experimentally measured energy levels.

The Landé interval rule is a useful spectroscopic metric, often employed for detecting deviations from the LS coupling, and the p^2

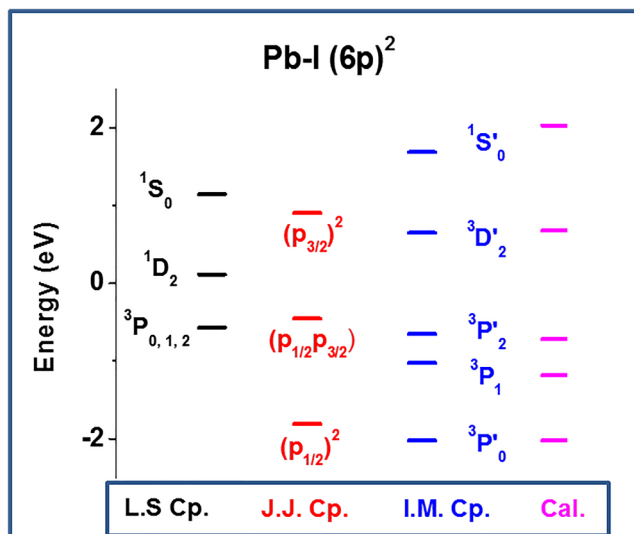


FIG. 3. Atomic energy levels of Pb as described within the LS , $j-j$, and intermediate coupling schemes together with the calculated ones. Data are taken from Ref. 7.

configuration is a typical textbook demonstration of it. Accordingly, for a pure LS -coupled atom, the separation between the energy levels of the resulting 3P sublevels with $J=2$ and $J=1$ should be two times that of the $J=1$ and $J=0$. For Si atom, these values are 0.018 and 0.0096, i.e., their ratio is very close to the expected ratio of 2. This ratio is almost 1 for Sn, indicating moderate deviation, but much smaller for Pb (0.36), indicative of a very strong deviation from LS coupling.

In Table II, we give again the experimental⁹ and theoretical relative energies (ΔE in eV), with the lowest level being set to 0, for the Pb atom. We also give the occupations of the $6p$ levels, $N(6p_{1/2})$ and $N(6p_{3/2})$, as obtained from the COSCI WFs for these levels. These occupation numbers are simply the expectation values of the orbital number operators over the COSCI WFs.⁴⁶ It should be noted that the occupation numbers are identical for all the states of the degenerate levels. This follows since the COSCI method provides exact multiplet WFs. Finally, we include the decomposition of the COSCI WFs into contributions from the different Russell-Saunders multiplets. These multiplets are obtained by projection of the

TABLE II. Composition of the different levels of Pb in terms of Russell-Saunders multiplets and $6p_{1/2}$ and $6p_{3/2}$ occupations. Comparison is made between theoretical and experimental multiplet splittings.

Level (J)	ΔE -expt ^a	ΔE -theory	%(3P)	%(1D)	%(1S)	$N(6p_{1/2})$	$N(6p_{3/2})$
1(J=0)	0.00	0.00	89.5	0.00	10.5	1.85	0.15
2(J=1)	0.97	0.83	100.0	0.00	0.00	1.00	1.00
3(J=2)	1.32	1.30	65.4	34.6	0.00	0.90	1.10
4(J=2)	2.66	2.70	34.7	65.3	0.00	0.10	1.90
5(J=0)	3.65	4.05	11.0	0.00	89.0	0.15	1.85

^aSee Ref. 9.

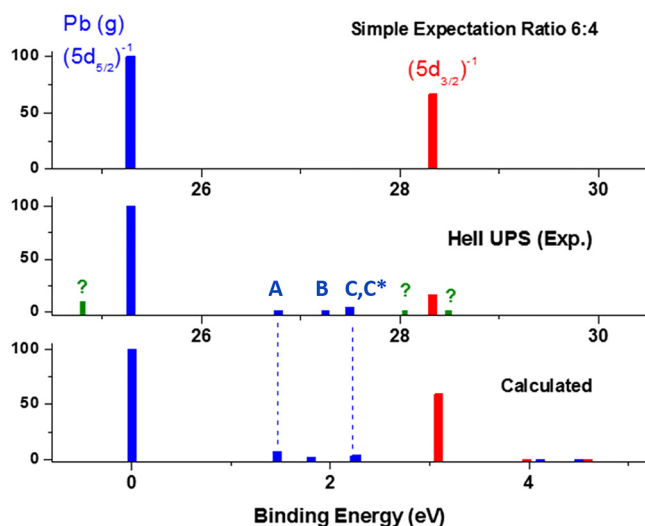


FIG. 4. Atomic Pb 5d PE spectrum together with calculated ones. Data are taken from Ref. 34.

Russell–Saunders multiplets calculated without spin–orbit splitting but only scalar relativistic effects on the solutions where spin–orbit splitting is included. For details of this projection, see Ref. 8. These decompositions are given as %(3P), %(1D), and %(1S).

As we have noted before, the lowest level is dominantly $(6p_{1/2})^2$ with only a 7.5% occupation of $(6p_{3/2})^2$; in terms of contributions from the Russell–Saunders multiplets, this level is 90% 3P_0 . The second level is a pure 3P_1 multiplet, but there is a considerable occupation of the spin–orbit split $6p_{3/2}$ orbital, which explains the higher energy of the multiplet from the ground $J = 0$ level. The first $J = 2$ level is a strong mixture of the Russell–Saunders 3P_2 and 1D_2 multiplets, while the second $J = 2$ level is dominantly, 95%, $(6p_{3/2})^2$. Figure 3 summarizes the different coupling schemes, together with the experimental and the calculated data.

B. Reassigning the He-II UV photoelectron spectrum of atomic Pb 5d manifold

Figure 4 displays the 5d spectrum of the Pb atom published in Ref. 34, together with our new relativistic calculations, and

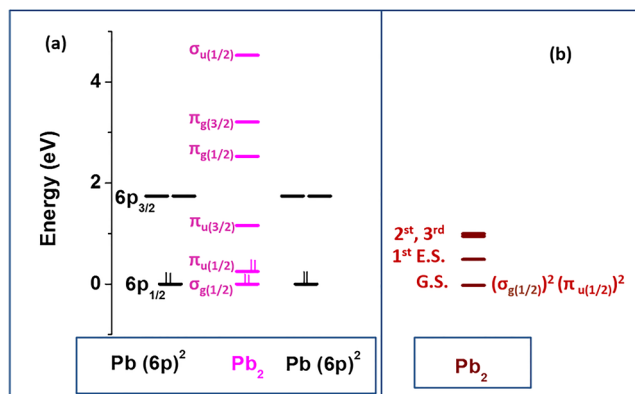


FIG. 5. Results of the Dirac–Fock calculations for atomic Pb and the Pb-dimer. (a) Schematics of atomic and molecular spinors. (b) The ground electronic configuration and three excited states of the Pb-dimer.

Table III gives the composition of the calculated ionic states in terms of their electron occupancy of the $5d_{3/2}$, $5d_{5/2}$, $6p_{1/2}$, and $6p_{3/2}$ spinors. For the 5d ion, the open shell configuration is $5d^9 6p^2$, and there are 16 multiplets with the XPS allowed J values of $3/2$ and $5/2$. In Fig. 4 and Table III, we only show the multiplets with relative SA intensity larger than 2, where the maximum intensity is normalized to 100. The calculations surprisingly reproduce energies of the observed spectral features and, to some extent, their relative intensities. Moreover, and as anticipated, the majority of the resultant ionic states like A, B, C, and C^* designated in the figure are admixture with almost one electron in both the $6p_{1/2}$ and $6p_{3/2}$ spinors of the valence level, i.e., strong reshuffling within the valence shell. However, there are three other experimentally observed weak peaks indicated as (?), which are still unassigned; there are no corresponding multiplets, even with low intensity, from our calculation.

As revealed in Table III, the lowest 5d ionized state reflects faithfully the compositions of the Pb atomic ground state, having a ratio of 1.84:0.16 $6p_{1/2}/6p_{3/2}$ occupancy ratio with one electron removed from the $5d_{5/2}$ sublevel. Other states correspond to shake-up states involving one $6p_{1/2}$ electron excited to the $6p_{3/2}$ level.

TABLE III. Calculated energy states of the 5d photoionized atomic Pb, and their occupancies with respect to 5d and 6p spinors.

Designation	Energy (eV)	Relative intensity	$5d_{3/2}$ occupancy	$5d_{5/2}$ occupancy	$6p_{1/2}$ occupancy	$6p_{3/2}$ occupancy
$(5d_{5/2})^{-1}$	0	100	4.00	5.00	1.84	0.16
A	1.47	7.0	3.90	5.10	1.00	0.92
B	1.80	3.0	4.00	5.00	1.00	1.00
C^a	2.24	3.4	3.93	5.07	1.03	0.97
C^*	2.26	4.2	4.00	5.00	0.94	1.96
$(5d_{3/2})^{-1}$	3.09	59	3.20	5.80	1.70	0.30

^aMultiplets C and C^* are combined in Fig. 4.

TABLE IV. Calculated energy states of Pb_2 , and their occupancies with respect to orbitals.

Formal designation	Relative energy (eV)	$\sigma_{g(1/2)}$ occupancy	$\pi_{u(1/2)}$ occupancy	$\pi_{u(3/2)}$ occupancy	$\pi_{g(1/2)}$ occupancy	$\pi_{g(3/2)}$ occupancy
$\sigma_{g(1/2)}^2 \pi_{u(1/2)}^2$ (G.S.)	0	1.84	1.80	0.14	0.16	0.034
$\sigma_{g(1/2)}^2 \pi_{u(1/2)}^1 \pi_{u(3/2)}^1$ (first E.S.)	0.51	1.76	1.02	0.90	0.19	0.062
$\sigma_{g(1/2)}^2 \pi_{u(1/2)}^1 \pi_{u(3/2)}^2$ (second E.S.)	0.95	1.00	1.83	0.94	0.14	0.074
$\sigma_{g(1/2)}^2 \pi_{u(1/2)}^2 \pi_{u(3/2)}^1$ (third E.S.)	1.00	1.02	1.75	0.94	0.14	0.020

C. Bonding properties of the Pb_2 -dimer

Pitzer and others had then commented on the changing trends in the bonding properties of group IV dimers, especially to a twofold decrease in the dissociation energy going from Sn_2 (1.90 eV) to Pb (0.86 eV) and attributable to poor bonding properties of $6p_{1/2}$ spinors.^{12,17–19} Therefore, as a further attempt for tracing the valence relativistic effects, calculations are performed for the lead dimer at the experimentally determined equilibrium bond length of the molecule at 2.93 Å.⁴⁷ Figure 5 displays, the energy levels of the ground states of two Pb atoms, and the corresponding relativistic molecular orbitals calculated for the dimer, which are also given in Table IV. From Table IV, the occupations of the different orbitals indicate the dominant configurations for the various states. Thus, the ground state is dominated by the configuration $\sigma_{g(1/2)}\pi_{u(1/2)}$, but it is not a pure single configuration for which the individual occupations would both be exactly 2. The second and third states are dominated by excitation from $\pi_{u(1/2)}$ to $\pi_{u(3/2)}$, while the third state is dominated by excitation from $\sigma_{g(1/2)}$ to $\pi_{u(3/2)}$.

A poor or nonexistent bonding property of the Pb -dimer is conveyed by our calculations, which is consistent both with Pitzer's predictions and also to some extent with the experimentally determined value of 0.86 eV. Most of this energy may be attributable to the van der Waals interactions, unaccounted by our calculations. Furthermore, the calculated energy difference between the ground and the first excited state of the dimer is 0.51 eV, which is also in very good agreement with the experimental energy difference of ~0.6 eV in the photodetachment electron spectrum of the same dimer reported in Ref. 47.

While writing the present paper, an earlier publication from Shirley's group has come to our attention. This paper had reported the XPS spectra of Tl , Pb , and Bi metals, recorded by $\text{Al-K}\alpha$ x rays. It had also pointed out that the valence band near the E_F of Pb -metal displayed a splitting of 1.8 eV and attributed it to the large spin-orbit splitting of the $6p$ valence level, rather than the crystal field effects.^{48,49}

V. CONCLUSIONS

Looking back to UC Berkeley days, S.S. appreciates much better (only afterward!) how Dave Shirley had created a warm, conducive, and vivid scientific melting pot, which without noticing had directed each and every member of his group to very quickly dwell on significant issues of scientific research, and his guidance has and will always be with us. One of us, P.S.B., also wishes to express his debt to Dave Shirley for having helped him understand

the complexities of XPS. This guidance drew him from the goal of performing calculations with state of the art numerical precision to performing calculations that provided a basis for understanding the physics and chemistry that were revealed by the XPS spectra. His first collaboration with Dave Shirley concerned multiplet splitting in the $3s$ XPS of MnO , which laid the foundation of our current understanding that multiple multiplets must be taken into account to properly assign the XPS of open shell systems.²¹

ACKNOWLEDGMENTS

P.S.B.'s contribution is based on work supported by the U.S. Department of Energy, Office of Science, Office of Basic Energy Sciences, Chemical Sciences, Geosciences, and Biosciences (CSGB) Division through its Geosciences program at the Pacific Northwest National Laboratory (PNNL). PNNL is a multiprogram national laboratory operated for the DOE by Battelle Memorial Institute under Contract No. DE-AC05-76RL01830.

AUTHOR DECLARATIONS

Conflict of Interest

The authors have no conflicts to disclose.

Author Contributions

P.S.B. and S.S. contributed equally to this work.

DATA AVAILABILITY

The data that support the findings of this study are available from the corresponding authors upon reasonable request.

REFERENCES

- K. S. Pitzer, *Acc. Chem. Res.* **12**, 271 (1979).
- P. Pyykko and J.-P. Desclaux, *Acc. Chem. Res.* **12**, 276 (1979).
- P. Pyykko, *Annu. Rev. Phys. Chem.* **63**, 45 (2012).
- N. C. Pyper, *Philos. Trans. R. Soc. London A* **378**, 20190305 (2020).
- S. Suzer, "High temperature UV photoelectron spectroscopy," Ph.D. thesis (University of California, Berkeley, 1976), LBL-Report 4922.
- S. Suzer, M. S. Banna, and D. A. Shirley, *J. Chem. Phys.* **63**, 3473 (1975).
- E. U. Condon and G. H. Shortley, *The Theory of Atomic Spectra* (Cambridge University, London, 1951).
- P. S. Bagus, M. J. Sassi, and K. M. Rosso, *J. Electron Spectrosc. Relat. Phenom.* **200**, 174 (2015).
- S. Suzer, Atomic Energy Levels, Natl. Bur. Stand. No. 467, U.S. GPO, Washington, DC, 1952; see also http://physics.nist.gov/cgi-bin/AtData/main_asd.
- J. P. Desclaux, *Int. J. Quantum Chem.* **6**, 25 (1972).

- ¹¹S. T. Lee, S. Suzer, and D. A. Shirley, *Chem. Phys. Lett.* **41**, 25 (1976).
- ¹²K. S. Pitzer, *J. Chem. Phys.* **63**, 1032 (1975).
- ¹³Y. Oganessian, *Radiochim. Acta* **99**, 429 (2011).
- ¹⁴V. Pershina, *Radiochim. Acta* **99**, 459 (2011).
- ¹⁵Ch. E. Dullman, *Radiochim. Acta* **100**, 67 (2012).
- ¹⁶A. Yakushev *et al.*, *Inorg. Chem.* **53**, 1624 (2014).
- ¹⁷K. Balasubramanian and K. S. Pitzer, *J. Chem. Phys.* **78**, 321 (1983).
- ¹⁸K. S. Pitzer and K. Balasubramanian, *J. Phys. Chem.* **86**, 3068 (1982).
- ¹⁹K. Balasubramanian, *Chem. Rev.* **90**, 93 (1990).
- ²⁰P. S. Bagus, Y. S. Lee, and K. S. Pitzer, *Chem. Phys. Lett.* **33**, 408 (1975).
- ²¹C. S. Fadley, D. A. Shirley, A. J. Freeman, P. S. Bagus, and J. V. Mallow, *Phys. Rev. Lett.* **23**, 1397 (1969).
- ²²P. S. Bagus, M. Schrenk, D. W. Davis, and D. A. Shirley, *Phys. Rev. A* **9**, 1090 (1974).
- ²³P. Pyykko, *Adv. Quantum Chem.* **11**, 353 (1979).
- ²⁴P. Pyykko, *Chem. Rev.* **88**, 563 (1988).
- ²⁵R. Ahuja, A. Blomqvist, P. Larsson, P. Pyykko, and P. Zaleski-Ejgierd, *Phys. Rev. Lett.* **106**, 018301 (2011).
- ²⁶P. Pyykko, *Chem. Rev.* **112**, 371 (2012).
- ²⁷L. J. Norby, *J. Chem. Educ.* **68**, 110 (1991).
- ²⁸F. Calleja *et al.*, *Nat. Phys.* **11**, 43 (2014).
- ²⁹I. J. Klimovskikh *et al.*, *ACS Nano* **11**, 368 (2017).
- ³⁰J.-J. Yang *et al.*, *JACS Au* **1**, 1178 (2021).
- ³¹D. Ma and Z. Yang, *New J. Phys.* **13**, 123018 (2011).
- ³²Y. A. Bychkov and E. I. Rashba, *JETP Lett.* **39**, 78 (1984).
- ³³P. S. Bagus, E. R. Batista, and R. L. Martin, in *Electronic Structure Theory of Plutonium Molecules and Compounds, Plutonium Handbook*, edited by D. J. Clark, D. D. Geeson, and R. J. Hanrahan (American Nuclear Society, LaGrange Park, IL, 2019), Vol. 4, pp. 2245–2271.
- ³⁴S. Suzer, *J. Chem. Phys.* **72**, 6763 (1980).
- ³⁵T. Saue *et al.*, *J. Chem. Phys.* **152**, 204104 (2020).
- ³⁶L. Visscher, O. Visser, P. J. C. Aerts, H. Merenga, and W. C. Nieuwpoort, *Comput. Phys. Commun.* **81**, 120 (1994).
- ³⁷G. Herzberg, *Molecular Spectra and Molecular Structure* (Van Nostrand, Princeton, 1950), Vol. I.
- ³⁸L. Visscher, H. J. Aa. Jensen, and T. Saue, with new contributions from R. Bast, S. Dubillard, K. G. Dyall, U. Ekström, E. Eliav, T. Fleig, A. S. P. Gomes, T. U. Helgaker, J. Henriksson, M. Iliaš, Ch. R. Jacob, S. Knecht, P. Norman, J. Olsen, M. Pernpointner, K. Ruud, P. Salek, and J. Sikkema, DIRAC, a relativistic *ab initio* electronic structure program, Release DIRAC08 (2008), see <http://dirac.chem.sdu.dk>.
- ³⁹K. A. Peterson, *J. Chem. Phys.* **119**, 11099 (2003).
- ⁴⁰See <http://www.tc.uni-koeln.de/PP/clickpse.en.html>.
- ⁴¹T. Aberg, *Phys. Rev.* **156**, 35 (1967).
- ⁴²R. Manne and T. Åberg, *Chem. Phys. Lett.* **7**, 282 (1970).
- ⁴³P. S. Bagus, C. J. Nelin, C. R. Brundle, B. V. Crist, N. Lahiri, and K. M. Rosso, *J. Chem. Phys.* **154**, 094709 (2021).
- ⁴⁴P. S. Bagus, E. S. Ilton, and C. J. Nelin, *Surf. Sci. Rep.* **68**, 273 (2013).
- ⁴⁵B. D. Hermsmeier, C. S. Fadley, B. Sinkovic, M. O. Krause, J. Jimenez-Mier, P. Gerard, T. A. Carlson, S. T. Manson, and S. K. Bhattacharya, *Phys. Rev. B* **48**, 12425 (1993).
- ⁴⁶L. D. Landau and E. M. Lifshitz, *Quantum Mechanics* (Addison-Wesley, Reading, 1958).
- ⁴⁷J. Ho, M. L. Polak, and W. C. Lineberger, *J. Chem. Phys.* **96**, 144 (1992).
- ⁴⁸L. Ley, R. Pollak, S. Kowalczyk, and D. A. Shirley, *Phys. Lett. A* **41**, 429 (1972).
- ⁴⁹L. Ley, R. A. Pollak, F. R. McFeely, S. P. Kowalczyk, and D. A. Shirley, *Phys. Rev. B* **9**, 600 (1974).